Fuel 326 (2022) 125096

Contents lists available at ScienceDirect

Fuel

journal homepage: www.elsevier.com/locate/fuel

Full Length Article

On the effects of NH_3 addition to a reacting mixture of H_2/CH_4 under MILD combustion regime: Numerical modeling with a modified EDC combustion model

Seyed Mahmood Mousavi [a], Freshteh Sotoudeh [a], Daeyoung Jun [a], Bok Jik Lee [a,*], Javad Abolfazli Esfahani [b], Nader Karimi [c,d]

[a] Institute of Advanced Aerospace Technology, Seoul National University, Seoul 08826, South Korea
[b] School of Mechanical Engineering, Pusan National University, Busan 46241, South Korea
[c] School of Engineering and Materials Science, Queen Mary University of London, London, E1 4NS, United Kingdom
[d] James Watt School of Engineering, University of Glasgow, Glasgow, G12 8QQ, United Kingdom

ARTICLE INFO

Keywords:
Ammonia combustion
NH_3-MILD combustion
Modified EDC combustion model
NO emission

ABSTRACT

This paper examines the behavior of reacting $NH_3/H_2/CH_4$ mixtures in moderate or intense low oxygen dilution (MILD) condition. A series of axisymmetric, turbulent reacting flow simulations are carried out incorporating a modified version of eddy dissipation concept and a few reaction mechanisms. The effects of adding a progressively increasing amount of NH_3 to a reacting H_2/CH_4 mixture in moderate condition are investigated. It is observed that addition of NH_3 to MILD combustion leads to markedly different behaviors compared to that in conventional combustion. Most notably, the inherently strong preheating of reactants in MILD combustion causes thermal cracking of NH_3 prior to ignition. The resultant production of H_2 profoundly affects the reacting flow as such increasing the NH_3 mass fraction in the fuel blend decreases the flame lift-off. Further, unlike that in conventional combustion, adding NH_3 to MILD combustion increases the process reactivity. In addition, the usual flame thickening typically seen in NH_3 flames is not observed here, while in keeping with the thermodynamic predictions, NH_3 addition lowers the temperature of combustion products. The results also show that in sharp contrast to that reported for conventional combustion, addition of NH_3 in MILD condition does not increase the emission of NO, while the mass fraction of NO_2 drops slightly. Overall, it is concluded that MILD combustion could be a promising route to NH_3 combustion.

1. Introduction

Ammonia (NH_3) as a carbon-free fuel has recently attracted considerable interest as the fuel of future with significant economic advantages [1]. This flammable inorganic substance is deemed to play a major role in decarbonization of the energy sector and development of H_2 economy. NH_3 consists of nearly 18% H_2 by mass and is recognized as contributing to H_2 combustion through a well-developed and economically viable transportation and storage infrastructure [1]. In contrast to pure H_2, NH_3 is transported relatively easily in liquid form. Also, the high octane number (about 130) of NH_3 helps eliminate knocking in internal combustion engines [2]. However, currently burning of NH_3 faces important challenges, which should be addressed before its extensive use in combustion systems. Amongst these, is the low combustion efficiency of NH_3 burning systems [2,3], originating from the low reactivity of NH_3 compared to hydrocarbons. Further, flame instabilities and high emissions of nitrogen oxides (NO_x) are observed during combustion of NH_3 [4-6]. The instabilities are chiefly due to the low flame speed of NH_3 [7,8], which leads to the flame blow-off and extinction [9]. Formation of NO in NH_3 combustion is primarily along the pathway of fuel NO and is much higher under lean conditions, requiring the employment of expensive post-treatment systems to reduce NO_x emissions [10,11]. However, while NH_3 can be burned in fuel-rich conditions to minimize emissions, this combustion regime demands removal of unburned NH_3 and other pollutants (N_2O) from the exhaust gases [10,11]. The issues of low flame velocity of pure NH_3 (~6–8 cm/s under stoichiometric conditions [12]) and high ignition energy [4] can be addressed by mixing NH_3 with other fuels to increase the reactivity of the unburned mixture [13]. Combustion of NH_3 and H_2

* Corresponding author.
E-mail address: b.lee@snu.ac.kr (B.J. Lee).

https://doi.org/10.1016/j.fuel.2022.125096
Received 24 January 2022; Received in revised form 20 June 2022; Accepted 23 June 2022
Available online 29 June 2022

Nomenclature

C_τ	fine structure volume constant
C_γ	residence time constant
CD_1, CD_2	coefficients of ECM
Da_η	Damköhler number at the Kolmogorov scale
L*	length scale
Re_T	turbulent Reynolds number
u^*	turbulent reacting fine structure characteristic velocity
S_T	turbulent flame speed
S_L	laminar flame speed
Y_i	mass fraction of the i^{th}

Greek letters

α	thermal diffusivity
α_T	Turbulent thermal diffusivity
γ_λ	fine structures mass fraction
τ^*	fluid mean residence time
τ_C	chemical time scale
τ_η	Kolmogorov mixing time scale
ε	turbulent dissipation rate
ν	Kinematic viscosity
$\dot{\omega}_i$	mean reaction rate of species i

Abbreviations

EDC	eddy dissipation concept
MILD	moderate or intense low oxygen dilution
ECM	energy cascade model

Superscripts

bar	time-averaged values
tilde	Favre-averaged values
*	Characteristics quantities

is an attractive way of achieving zero-carbon combustion while improving combustion performance (flammability and stability).

In a spark-ignition engine, Mørchet al. [14] examined the combustion of NH_3/H_2 mixtures. They discovered that a high H_2 mass fraction in the mixture and an excess air ratio range between 1.1 and 1.4 resulted in greater NO_x emissions. It was also found that NO_x levels could be reduced to those of gasoline combustion through post-combustion destruction, implying that NH_3/H_2 mixtures could be an alternative to hydrocarbons in spark ignition engine. An analysis of burning NH_3/H_2 blended fuels in a porous burner was carried out by Nozari et al. [15]. The porous burners were found capable of burning fuel blends with a significant fraction of NH_3. In a swirl burner, Valera-Medina et al. [16] studies combustion of NH_3/H_2 and NH_3/CH_4 mixtures. These authors discovered that the NH_3/H_2 fuel blends had a limited equivalence ratio ranges for which the flames stayed stable, and that NO_x emission might overtake the maximum levels of 4500 ppm. The flame stability was attained for a wider equivalence ratio ranges in the NH_3/CH_4 fuel mixtures, whereas NO_x emission might reach a maximum levels of 2600 ppm near stoichiometry. In a gas turbine, Kurata et al. [11] investigated combustion of NH_3 as well as NH_3/CH_4 blends. It was reported that the NO_x emission for pure NH_3 combustion was the lowest, barely around 1000 ppm. Moreover, they hypothesized that the separation of rich and lean zones inside the burner caused an interaction between unburned NH_3 and NO_x, lowering the overall NO_x emissions. Consequently, however, a large NH_3 concentration (more than1500 ppm) emerged at the combustion chambers outlet. The burning of NH_3/CH_4 fuel mixtures, on the other hand, resulted in significantly lower NH_3 emissions. Rocha et al. [17] described a study of NH_3/H_2/air ignitions, premixed flame propagations, and NO emissions using chemical kinetic modeling. They showed that NH_3 combustion could feature long ignition delays and low flame speeds and that adding H_2 to the process could enhance the flame speed significantly with the expense of major increases in NO_x emissions.

Han et al. [18] studied the laminar firing rates of NH_3/air, NH_3/H_2/air, NH_3/CO/air, and NH_3/CH_4/air combustions by the heat flux methodology to better understand the properties of NH_3 combustion. Blending NH_3 with H_2 has been proven to be an effective way of boosting the flame speed of NH_3-based fuel mixtures. Ramos et al. [19] investigated NH_3, CO, and NO emissions from premixed NH_3/CH_4/air flames. They discovered that NO_x emissions increased with the NH_3 molar fraction up to 0.5 before they diminish. Furthermore, NO_x emissions dropped when the equivalence ratio decreased toward fuel-lean settings, but CO and NH_3 emission remained relatively low regardless of the operating conditions. Analyses of premixed swirl flames fed with NH_3/H_2 blends under very-lean to stoichiometric conditions was reported by Zhu et al. [20]. These authors showed that the OH* chemiluminescence level could be utilized as a proxy for the NO mole fraction under certain conditions. Based on the weak flame responses recorded in a micro flow reactor with a controlled temperature profiles, Murakami et al. [21] evaluate the influence of blending and equivalence ratio on the oxidation and reactivity of dimethyl ether/NH_3 blends. As the NH_3 mass fraction in fuel mixture increased from 0 to 15%, dimethyl ether oxidation was boosted and mixture reactivity increased under stoichiometric condition. CO oxidation was inhibited when the NH_3 mass fraction increased from 15 to 50%, and the mixed reactivity were significantly reduced. At intermediate temperatures of 800–1000 K, NO_x generated by NH_3 oxidation enhanced the reactivity of radicals via the NO–NO_2 catalytic loop.

The other practical approach to using NH_3 as a fuel for power generation is the application of the well-demonstrated concept of MILD combustion. This offers the unique potential to increase combustion performance while at the same time reducing pollutant emissions [22,23]. In general, MILD regime includes preheating and dilution, which boost flame stability and decrease thermal NO_x emission [22]. The concept of MILD combustion shares some of its fundamental features with modern engine technologies, such as homogeneous charge compression ignition and exhaust gas recirculation. It should be noted that MILD combustion technology can adapt to the complexity and variability of power consumption patterns while avoiding drastic changes in existing power plants [24].

Some recent studies have shown the potential for using carbon-free fuels such as NH_3 or NH_3/H_2 mixtures with promising results for MILD combustion. For instance, Manna et al. [25] experimentally characterized NH_3 oxidation and pyrolysis processes in model reactors. In the jet stirred flow reactor, the data obtained allowed for the identification of three distinct kinetic regimes in NH_3 oxidation: low temperatures ($T_{in} < 1130$ K), middle temperatures ($1130 < T_{in} < 1250$ K), and high temperatures (T_{in} greater than 1250 K). Surface heterogeneous reactions appeared to have no influence on NH_3 reactivity and H_2 profiles, but they did have an effect on NO_x concentration in the low-intermediate temperature range. Sue et al. [26] experimentally showed that NH_3-MILD combustion decreases NO_x emissions by a substantial amount. Sabia et al. [27] reported that NH_3/CH_4 mixtures are important when biogas is used as a fuel, and MILD combustion could represent an important solution to keep NO_x emissions very low.

Ferrarotti et al. [28] developed an innovative, multidisciplinary technique for analyzing NH_3/H_2 mixtures in flameless combustion. They demonstrated that adding a trace quantity of NH_3 to pure H_2 significantly boosted NO emissions (10% by volume). When operating at sufficiently close to stoichiometric circumstances (equivalence ratio of

0.95), an optimal trade-off between NO_x emission and NH_3 slip was discovered. According to these authors, enlarging the air injector could cut down the emissions. When the equivalence ratio of 0.8 was reached, emissions were reduced further more. Sorrentino et al. [29] studied the stability and emission features of the NH_3-MILD regime for several equivalence ratios and inlet temperatures. They reported lower NO_x levels close to the stoichiometric condition and stable combustion at above 1300 K. Ariemma et al. [30] examined the behavior of H_2O-assisted NH_3-MILD combustion under both premixed and non-premixed conditions. Their findings showed that H_2O addition to the combusting flow in the NH_3-MILD regime is a very simple and efficient way of reducing NO emissions in the fuel-lean MILD regime. Rocha et al. [31] conducted numerical simulations of an idealized combustor and observed that MILD combustion could produce minimal NO_x (50 ppm) and unburned NH_3 (0.1 ppm) emissions. The authors did highlight, however, achieving this requires a large amount of exhaust gas recirculation, which might be unfeasible. Sorrentino et al. [32] analyzed the reactive structure of a one-dimensional steady NH_3-counter flow diffusion flame. These authors indicated that in comparison with the case of fuel preheating, NH_3-MILD combustion is more stable at lower fuel dilution levels when the oxidant flow is preheated. Ariemma et al. [33] concentrated on the NH_3/CH_4-MILD combustion in a lab-scale burner in order to examine the gaseous pollutant emissions and stability of the process limitations as a function of the equivalence ratio and the NH_3/CH_4 ratio. It was shown that compared to pure NH_3, the use of NH_3/CH_4 mixtures could make the system much more stable in terms of working temperatures and equivalence ratios. However, utilization of fuel blends resulted in greater NO_x emissions as compared to those emitted by pure NH_3 and CH_4. Zhao et al. [34] explored the role of co-flow O_2 and temperature on MILD combustion and fuel-NO mechanism of CH_4/NH_3 jet diffusion flames in hot O_2/CO_2 co-flow. Temperature and co-flow O_2 were varied from 3% to 30% and 1300 K to 2100 K, respectively. The results indicated that when co-flow O_2 was 21%, MILD-oxy combustion could be fully achieved for all co-flow temperatures. However, a higher co-flow temperature was required to maintain MILD regime when co-flow O_2 was 24%. Sun et al. [35] examined the homogeneous oxidation of $CH_4/NH_3/NO/NO_2$ mixtures at temperatures ranging from 600 K to 1200 K in a laminar flow reactor under atmospheric pressure. The results indicated that when NH_3/NO_x mixtures were oxidized, the NO/NO_2 ratio affected the conversion of NO via the reaction $NH_2 + NO_2 = H_2NO + NO$. The inclusion of CH_4 considerably increased the oxidation reactivity of the NH_3/NO_x combination. As the amount of CH_4 added rose, the generation of H_2O increased while the synthesis of N_2 dropped. Furthermore, when $CH_4/NH_3/NO_x$ mixtures were oxidized, the NO_2/NO ratio had little influence on the generation of main products and intermediates. Manna et al. [36] studied the oxidation of highly diluted NH_3-H_2 mixtures at low-intermediate temperatures in a jet stirred flow reactor. In a parametric study, they varied the mass fraction of H_2 in the fuel blend, the mixture equivalence ratio, and the inlet temperatures. It was observed that H_2 addition barely improved the system reactivity at low-intermediate temperatures and pushed lower reactivity and dynamic regimes toward lower reactor temperatures.

Studies on NH_3 combustion in conventional conditions have already revealed the requirement for highly swirling burners to increase stability and minimize nitrogen oxide emissions. Therefore, MILD combustion might be considered as the asymptotic solution to the problem. Literature indicates that gains in performance in terms of efficiency and flexibility could emerge. Nevertheless, a rigorous study on this topic has not been reported yet. Therefore, the focus of the current work is on $NH_3/CH_4/H_2$ mixtures, with relatively high mole fraction of CH_4, to gain a profound understanding of the effects of NH_3 on the main parameters of MILD combustion. These include preheating zone length, flame front, the thickness of the reacting zone as well as NO_x and CO emissions. A Dally's burner, like the one used in earlier studies [37,38], was used for the current investigation. In general, the difficulty of simulating this regime has been one of the key challenges, stemming from the uncommon interactions between transport and chemistry in MILD combustion [39,40]. To resolve this issue, several modeling approaches have already been proposed [41-45]. According to the flow conditions in the present work and findings of the previous studies, the method presented by Cuoci et al. [46,47] seems to be the most appropriate. Hence, in the proceeding study the extended edcSimpleSMOKE solver, proposed by this group is employed with different reaction mechanisms and k-ε turbulence model.

Numerical method.

1.1. Eddy dissipation concept

The eddy dissipation concept (EDC) [23] is useful for the prediction of turbulent reacting flows, especially in the modes in which combustion kinetics play an important role (e.g. MILD combustion) [48,49]. An energy cascade model (ECM) provides the fine structures mass fraction (γ_λ) and the fluid mean residence time (τ^*) [32]. To calculate the residence time, there are two constants including the fine structure volume and residence time constants. These are set to 2.137 and 0.4083 by default. Based on the classical ECM, the fine structure scale is of the same order of the Kolmogorov scale as follows;

$$Re^* = \frac{u^* L^*}{\nu} = \frac{2}{3}\frac{C_{D2}}{C_{D1}} = 2.5 \tag{1}$$

It should be noted that this model is appropriate for high Reynolds number flows in which there is a significant distinction amongst turbulent scales. There is no apparent distinction between turbulence on large and small scales in MILD conditions, and reactions occur across a wide range of scales [47]. Consequently, the chemical reaction proceeds in a thick reaction region that corresponds to the integral length scale. This modifies the characteristic scale of the reaction structure because energy is transferred at a higher frequency than that of the reaction structure in the spectrum [50]. Hence, it is essential to consider the nature of MILD combustion mode and modify the cascade model. This is also needed to explain how the ECM parameters are affected by the flow and response qualities represented by the Reynolds and Damköhler numbers. Dilution and preheating of oxidizer under MILD condition create a unique distributed reaction area [47]. Damköhler number about one characterizes the system evolving towards the perfectly mixed condition. Parente et al. [47] modified the classical cascade model by assuming that MILD condition occurs in the so-called 'Distributed Reaction Regime' with small-scale and high-intensity turbulence. They noted that the use of Eq. (15) could be a good first-order approximation for the characteristic velocities of the reaction structure for MILD condition. Further, it could be utilized to derive the dependency of the coefficients of ECM (CD_1 and CD_2) on the dimensionless number of combusting flows.

$$S_T \approx S_L\sqrt{\frac{\alpha_T + \alpha}{\alpha}} \approx S_L\sqrt{Re_T + 1} \tag{2}$$

The relation between the turbulent dissipation rate and turbulent reacting fine structure characteristic velocity (u^*) indicates.

$$\varepsilon \propto C_{D2}\nu u^{*2}/L^{*2} \tag{3}$$

where $u^* \approx S_T \approx S_L\sqrt{Re_T + 1}$. Combination of Eqs. (2) and (3) leads to the following definition;

$$\varepsilon \propto C_{D2}\nu\frac{u^{*2}}{L^{*2}} = C_{D2}\nu\frac{S_L^2(Re_T + 1)}{L^{*2}} \tag{4}$$

in which, L^*/S_L is the characteristic chemical time scale (τ_C) of the reaction structure according to the classical treatment of a turbulent premixed flame [36]. Therefore, τ_C is expressed as a function of the Kolmogorov mixing time scale (τ_η) by the Damköhler number of reacting flow. Thus, the dissipation is defined as:

$$\varepsilon \propto \frac{[C_{D2}\nu(Re_T+1)]}{\tau_c^2} = \frac{[C_{D2}\nu(Re_T+1)Da_\eta^2]}{\tau_\eta^2} \quad (5)$$

Here, $Da_\eta = \tau_\eta/\tau_c$ is Damköhler number which has a value of one in MILD condition. Based on$\tau_\eta = (\nu/\varepsilon)^{\frac{1}{2}}$, the dependency of C_{D2} on Re_T and Da_η is obtained as below

$$C_{D2} \propto \frac{1}{[Da_\eta^2(Re_T+1)]} \quad (6)$$

Also,

$$C_\tau \propto \frac{1}{Da_\eta\sqrt{Re_T+1}} \quad (7)$$

A similar method for determination of the dependency of C_γ on Re_T and Da_η leads to the following definition

$$C_\gamma = \left(\frac{3C_{D2}}{4C_{D1}^2}\right)^{\frac{1}{4}} \propto \left[\frac{(Re_T+1)}{C_{D2}}\right]^{\frac{1}{4}} \propto Da_\eta^{\frac{1}{2}}(Re_T+1)^{\frac{1}{2}} \quad (8)$$

1.2. Plug flow reactor

Disregarding mixing term between the fine structures and their surroundings is a straightforward technique to eliminate the instabilities and reducing the computational burden [51,52]. Since back-mixing is neglected in the species conservation equations and only chemistry is integrated over time, this technique is referred to as the plug flow reactor approach. A plug flow reactor is a one-dimensional, steady-state reactor that has both inflow and outflow, as well as a distribution of characteristics along the flow direction. In this technique, reactions occur across time scales dictated by Arrhenius rates. When the flow velocity, area, and pressure are constant, the governing equations may be translated into transient equations, such as the species mass balance, which can be written as:

$$\frac{dY_k}{dt} = \frac{R_k^*}{\rho^*} \quad (9)$$

The initial conditions are considered as the current species and temperature in the cell meaning that Eq. (9) is integrated from $Y_k(t=0) = \widetilde{Y}_k$to $Y_k(t=\tau^*) = Y_k^*$.

Numerical settings, configuration, computational grid and boundary conditions.

The OpenSMOKE library [46] and the extended edcSimpleSMOKE solver [53] with a simple algorithm in a two-dimensional axisymmetric configuration were used in this study to detect the physics of MILD combustion in several working conditions. Table 1 shows the details of the present numerical set-up. In the present work, the turbulent Prandtl number value was set to one. The existing experimental data [54] for a typical Jet-in-Hot-Coflow burner (Dally burner) with the configuration shown in Fig. 1 was used to validate the results of the extended EDC model [54,55]. Dally's burner contains a hot co-flow and a fuel inlet nozzle with the diameters of 80 and 4.25 mm, respectively. It should be noted that the burner is equipped with a wind tunnel with a diameter of 420 mm. In the tunnel, air flows at a speed of 3.2 m/s in a direction parallel to the burner axis [56]. Table 2 indicates the working conditions considered in the current simulations. For the current MILD combustion problem, H_2, CH_4, N_2, H_2O, and CO_2 are the main components of the inlet flows. Furthermore, H_2/CH_4 fuel is injected with the inlet Reynolds number of 10,000. It is noted that the velocity inlet and pressure outlet boundary conditions were set for the upstream and downstream, respectively.

Table 1
Numerical setup for the simulations in the present work.

Code	OpenFOAM-7
Solver	Modified edcSimpleSMOKE
Combustion model	EDC
Multicomponent diffusion	yes
Molecular viscosity	Sutherland law
Coupling of Pressure and velocity fields	SIMPLE
Schemes of discretization	second order
Fine structure reactor	Plug fine structure
Turbulent Schmidt number	0.7
Turbulent Prandtl number	1.0
mechanism of chemical reaction	GRI-Mech 3.0

It has been already shown that the turbulence intensity of the hot co-flow and inlet nozzles did not affect the solution [37,38,55,57,58]. Yet, the fuel inlet turbulence intensity is important [38]. Christo et al. [55] observed that the mean turbulent kinetic energy of 60 m^2/s^2 at the fuel inlet yields the best agreement between the simulations and experimental data for the distribution of species mass fraction and temperature.

Furthermore, the grid sensitivity analysis is depicted in Fig. 2. Three cell configurations of 11000, 33000, and 99,000 cells elements were employed to assess the grid independency of the numerical solutions. The results for the mass fractions of CH_2O and OH radicals are shown in Fig. 2. According to the data in this figure, the relative differences between the results of 33,000 and 99,000 elements are approximately 0.2%, indicating that the results are independent of the grid for the cell configurations with more than 33,000 elements. As a result, this grid was employed for the rest of the investigations reported in this study.

Moreover, as shown in Fig. 1, a finer mesh around the fuel and co-flow inlets was employed, with high grid resolution in the reaction region to moderate the computational cost. Note that, in Fig. 1, there are 6 lines by the axial distances of 5 (L1), 10 (L2), 15 (L3), 20 (L4), 25 (L5), and 30 (L6) cm to compare different cases.

1.3. Validation

This section presents validation of the numerical simulations by comparing the detected radial mass fraction with the experimentally determined temperature distributions [54] at the axial distances (ADs) of 30 and 120 mm. For this purpose, two different approaches, including the EDC method with default values and modified-EDC with modification of C_{D1} and C_{D2} coefficients as in Eqs. (1)–(8), were used. Fig. 3 illustrates a comparison between the predicted results and the experimental data [54] for the radial distributions of OH, CO, and H_2O as well as those of temperature at the ADs of 30 and 120 mm from the inlet. The default-EDC model is clearly incapable of forecasting the distribution of chemical species and the maximum temperature, as this model could not detect the local extinctions and predict the characteristics of MILD combustion like reaction zone thickness. However, due to the physical properties of MILD combustion, this model has a large error in predicting CO and OH species, as also reported by other researchers [59,60]. This is due to the cooling and extinction influences of the premixed reacting flow inside the secondary combustion chamber where the behavior of the reacting flow deviates from the MILD condition [55,60]. In general, due to the importance of these two species in combustion process, the use of an EDC model is not recommended. However, by changing C_{D1} and C_{D2} coefficients to 0.167 and 1, satisfactory agreement was found between the simulations and the experimental results. The increase in C_{D1} and C_{D2} coefficients enhances the time coefficient of fine structure. This means that, considering the wider reaction zones, smoother gradients exist to reduce the driving forces and lower the temperature with the higher dilution. The characteristics of MILD combustion were recently analyzed by Minamoto et al. [34], who found that the reaction region in this regime was distributed over a considerable part of the burner. Further, the interactions amongst the reactive regions both distribute these zones and uniform the temperature distribution. In this case, u' has a significant effect on the combustion process, and Kolmogorov scales have the ability to enter and widen the preheating region, as well as the reacting area, resulting in a

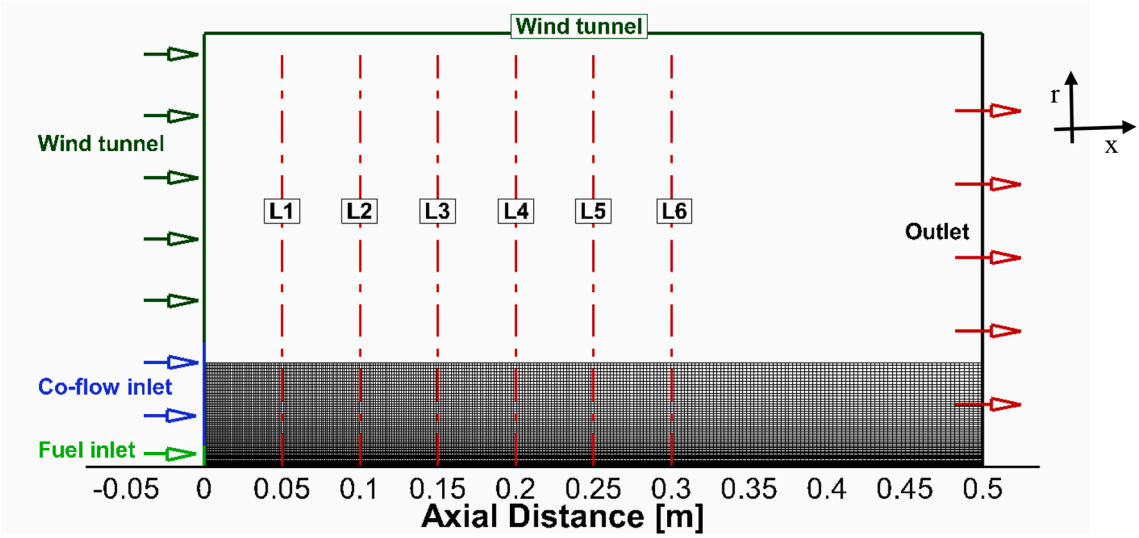

Fig. 1. Schematic view of computational domain and cell configuration.

Table 2
Working conditions considered in the simulations [54].

Inlet condition	Fuel	Co-flow	wind Tunnel
Composition, mass fraction	$H_2 = 11.1$, $CH_4 = 89.9$	$O_2 = 9$, $N_2 = 79$, $H_2O = 6.5$, $CO_2 = 5.5$	$O_2 = 23.3$, $N_2 = 76.7$
Temperature [K]	300	1300	300

thicker and diffused flame. [61]. By increasing the role of u', Re_T increases, leading to an increase in the fine structure coefficient (with a lower percentage than the fine structure time coefficient). Considering these parameters and characteristics, the modified-EDC model can accurately predict the structure of MILD combustion in both centerline of the burner and radial distance in various ADs. In addition, the following equation [62] was used for calculating the error of the present work in predicting the experimental data. Using Eq. (10) shows that the average values of numerical results accuracy in predicting H_2O, CO, OH, and temperature are 96.5, 97.3, 97.3, and 97.6%, respectively.

$$R^2 = \frac{\sum_{i=1}^{n}\left(Z_{\exp,i} - Z_{simulation,mean}\right)^2 - \sum_{i=1}^{n}\left(Z_{\exp,i} - Z_{simulation,i}\right)^2}{\sum_{i=1}^{n}\left(Z_{\exp,i} - Z_{simulation,mean}\right)^2} \quad (10)$$

Next, the capability of the GRI-Mech 3.0 in predicting the behavior of MILD combustion with NH_3 added to the fuel blend is investigated. There exist several reaction mechanisms which include NH_3 [63,64]. Importantly, however, most of them are restricted to the mixtures of H_2 and NH_3. Further, the chemical mechanisms of $CH_4/H_2/NH_3$ by Okafor et al. [65], $NH_3/H_2/CH_4$-R1 [60], and $NH_3/H_2/CH_4$-R2 [60], by the characteristics shown in Table 3, have been used. The fuel compositions in this section include $H_2 = 11.1$, $CH_4 = 69.9$, and $NH_3 = 20$ (NH20 case in Table 4), with the inlet velocity and temperature, as well as the inlet co-flow and wind tunnel characteristics as those described in Table 2. Fig. 4 shows a comparison among the outcomes of these four mechanisms for different species and the process temperature at different axial locations. It is observed that using the GRI-Mech 3.0 mechanism, similar results are obtained to those of other mechanisms. This is because the mass fraction of CH_4 in the investigated blend is much greater than that

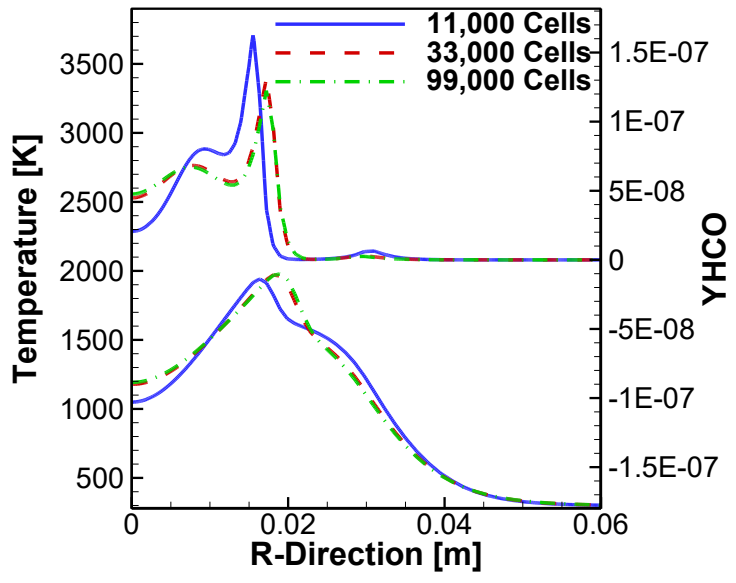

Mesh elements	Relative error %
11,000	17
33,000	0.2
99,000	-

Fig. 2. The grid independency tests.

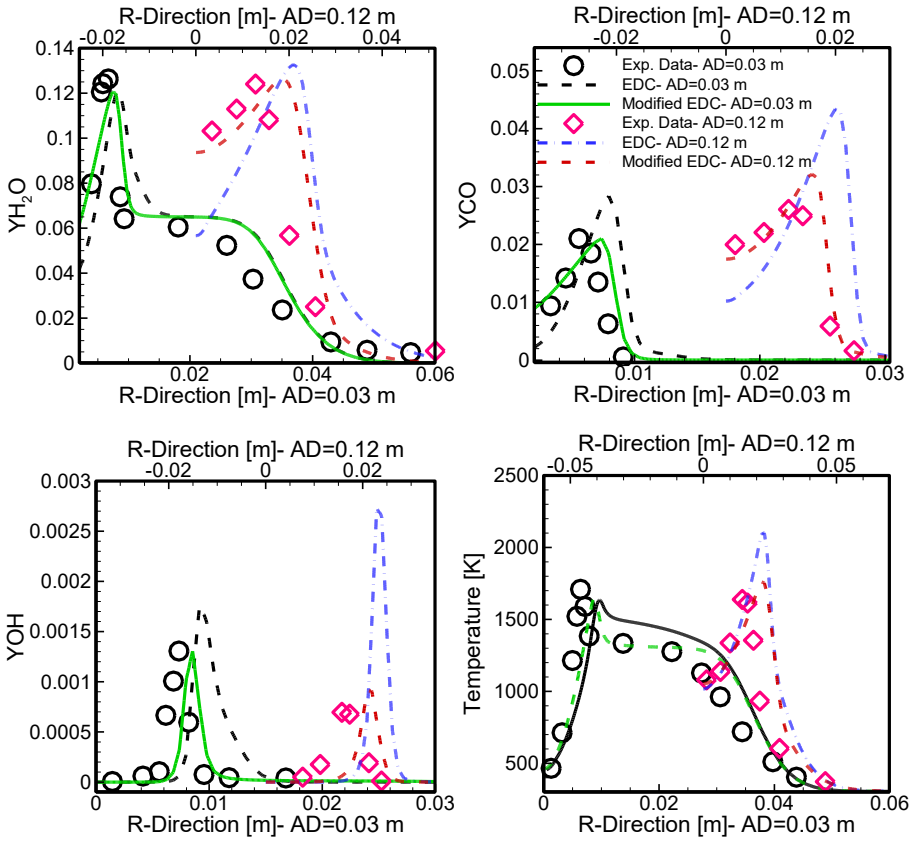

Fig. 3. Comparison between the current simulations and the experimental data of Ref. [54].

Table 3
The main characteristics of the reaction mechanisms used in the present work.

Reaction mechanism	Okafor et al. [65] (M1)	GRI-Mech 3.0 [66] (M2)	$NH_3/H_2/CH_4$-R2 [60] (M3)	$NH_3/H_2/CH_4$-R1 [60] (M4)
Number of reactions	130	325	420	634
Number of species	42	53	51	74

Table 4
Mass fraction of the inlet fuel composition ($H_2/CH_4/NH_3$).

Inlet condition	Mass fractions of H_2, CH_4 and NH_3 in the reactants
NH0	$H_2 = 11.1$, $CH_4 = 88.9$, $NH_3 = 0$
NH5	$H_2 = 11.1$, $CH_4 = 83.9$, $NH_3 = 5$
NH10	$H_2 = 11.1$, $CH_4 = 79.9$, $NH_3 = 10$
NH15	$H_2 = 11.1$, $CH_4 = 73.9$, $NH_3 = 15$
NH20	$H_2 = 11.1$, $CH_4 = 69.9$, $NH_3 = 20$

of NH_3. It was observed that when the molar fraction of NH_3 was pushed greater than 30% and that of CH_4 was lower than 50%, the results of GRI-Mech 3.0 were quite different from the results of the other NH_3 mechanisms. Furthermore, it is noted that the majority of reactions in the Okafor mechanism [64] are from the GRI-Mech 3.0 mechanism. It follows that the use of the GRI-Mech 3.0 mechanism is acceptable for the blends with low concentration of NH_3.

2. Results and discussions

This section presents the effects of adding NH_3 with various mass fractions on the behavior of MILD combustion in the configuration shown in Fig. 1. To this end, four different cases shown in Table 4 were considered. It is noted that the other inlet conditions such as inlet temperatures, velocities, and mass fractions, are the same as those presented in Table 2.

Fig. 5 shows the preheating zone in which $T \leq T_{self\ ignition}$, before reaching the maximum H_2 and CO mass fraction [61], and no reactions take place, for MILD combustion of $NH_3/CH_4/H_2$. This figure is drawn in the direction of the starting point of the reaction, which is higher than the centerline, and it includes the results for different mass fractions of NH_3 in the fuel blend. Due to the low reactivity and burning velocity of NH_3, thicker flames are often formed in conventional combustion. Per unit mass, NH_3 has a much lower enthalpy of combustion compared to methane. Therefore, compared to CH_4, NH_3 combustion is projected to generate lower temperatures. However, as Fig. 6 shows, H_2 is produced by the thermal decomposition of NH_3 in the zone near the inlet nozzle. Evidently, increasing the mass fraction of NH_3 in the fuel component leads to an increase in the H_2 mass fraction before the axial distance of 0.07 m. Beyond this point, the burning rate increases because of the enhancement of H_2, and the mass fraction of H_2 drops by increasing the mass fraction of NH_3. This is because the preheating temperature in MILD combustion exceeds that needed for the thermal cracking of NH_3 (NH_3 thermal cracking occurs at 1200 K [67,68]). As a result, the ignition delay is reduced while the decomposition of NH_3 increases the reaction rate. In addition, blending NH_3 with H_2 and CH_4 results in an enhancement of flame speed and process heat release. Therefore, using NH_3 in MILD condition shortens the preheating zone, as shown in Fig. 5. Based on this figure, as the mass fraction of NH_3 increases from 0 to 20%, the preheating length reduces by up to 85%. However, it should be noted that the preheating zones for NH15 and NH20 are approximately the same length. This behavior is further illustrated in Fig. 7, in which the distribution of OH mass fraction has been plotted as a function of NH_3 mass fraction. The OH free radical is an indicator of heat release from the combustion process and it also marks the reacting zone [69]. Evidently,

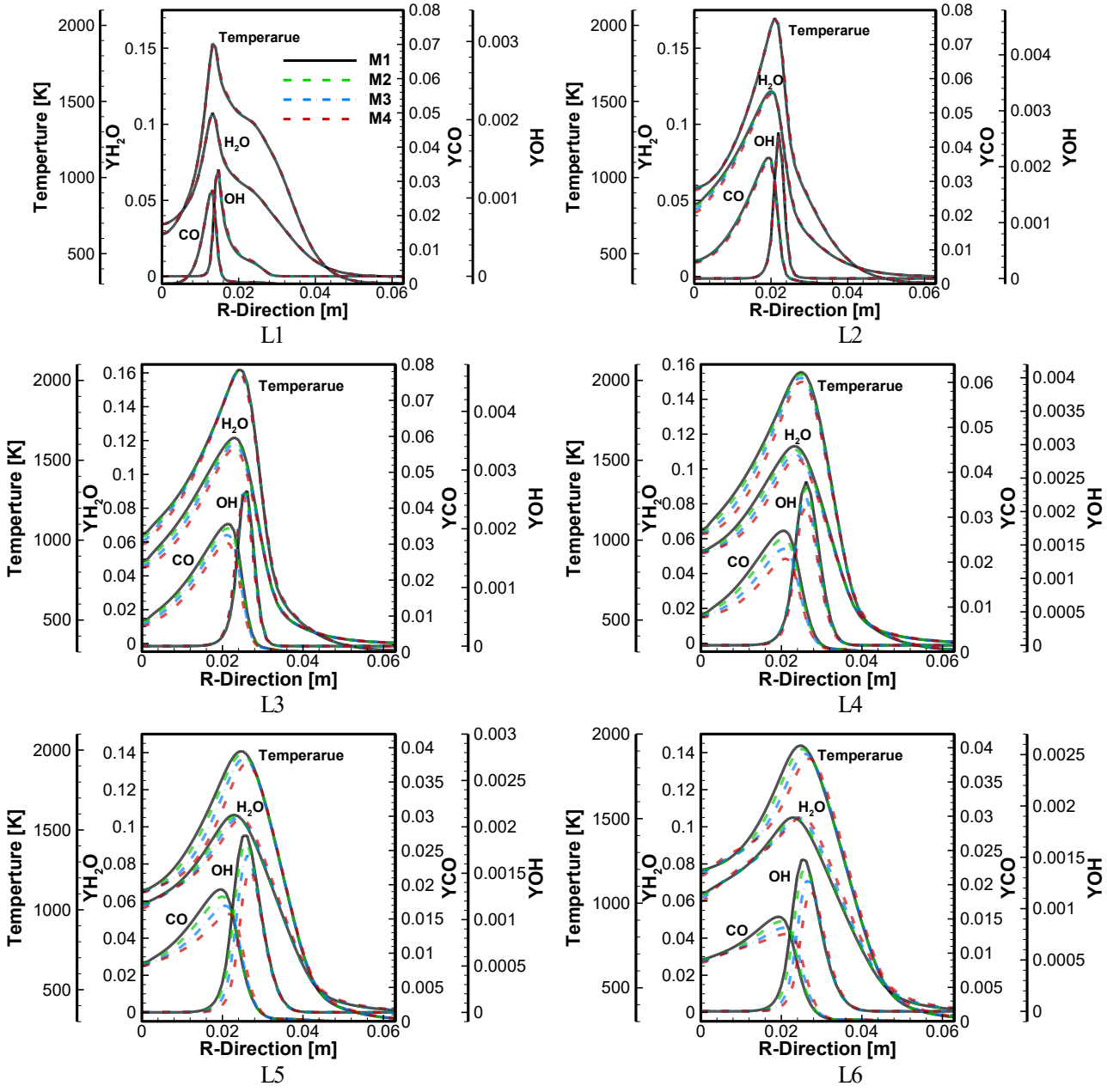

Fig. 4. Comparison among the results of Okafor et al. (M1), GRI-Mech 3.0 (M2), $NH_3/H_2/CH_4$-R2 (M3), and $NH_3/H_2/CH_4$-R1 (M4) mechanisms.

increasing the NH_3 mass fraction in the blended fuels moves the starting point of OH radical production toward to the inlet nozzle, and unlike that in conventional combustion, the addition of NH_3 to MILD combustion increases the process reactivity.

At various axial distances, Fig. 8 depicts the radial variation of OH mass fraction as a flame marker. The low laminar flame speed of NH_3 contributes to the increases in the thickness of the reaction zone. However, based on this figure increasing the NH_3 mass fraction in the blended fuel decreases the thickness of the reacting zone in MILD condition. There are two reasons for such behavior, 1) preheating temperature higher than the thermal cracking temperature of NH_3, and 2) blending NH_3 with CH_4 and H_2, which increases the flame speed with respect to the NH_3 combustion without H_2/CH_4. When comparing the amount of OH at various dilution levels, there is a competition between the rate at which the temperature falls when NH_3 is added and the rate at which H is added when ammonia is cracked. In this regard, Fig. 8 shows that the localized OH mass fraction is reduced by up to 8.3% in the NH20 case in comparison with NH0. This is attributed to the reduction of temperature in NH20, which is about 80 K compared with NH0 (Fig. 11) due to an overall increase in the nitrogen content of the mixture. Further, adding NH_3 and reduction of CH_4 in the fuel component increase the overall H production in the mixture due to cracking (Fig. 15) which is the other reason for the reduction of OH radical. This confirms that the flame becomes weaker with increasing the NH_3 mass fraction.

In general, the phenomena related to decreases in the OH free radical have been explained as a "weakening" of the flame front [70]. The weakening of the reaction zone is primarily attributted to the rate of heat release, which is marginally impacted by the high temperature of the coflow and shear layer mixing. Fig. 9 demonstrates the zone of maximum mass fraction of OH for various values for the cases stated in Table 4. The yellow color in the cadres shows the maximum value of the OH radical. Evidently, increasing the mass fraction of NH_3 in the fuel component, followed by a decrease in the mass fraction of CH_4, results in a reduction in the area and thickness of these zones. Since OH radical

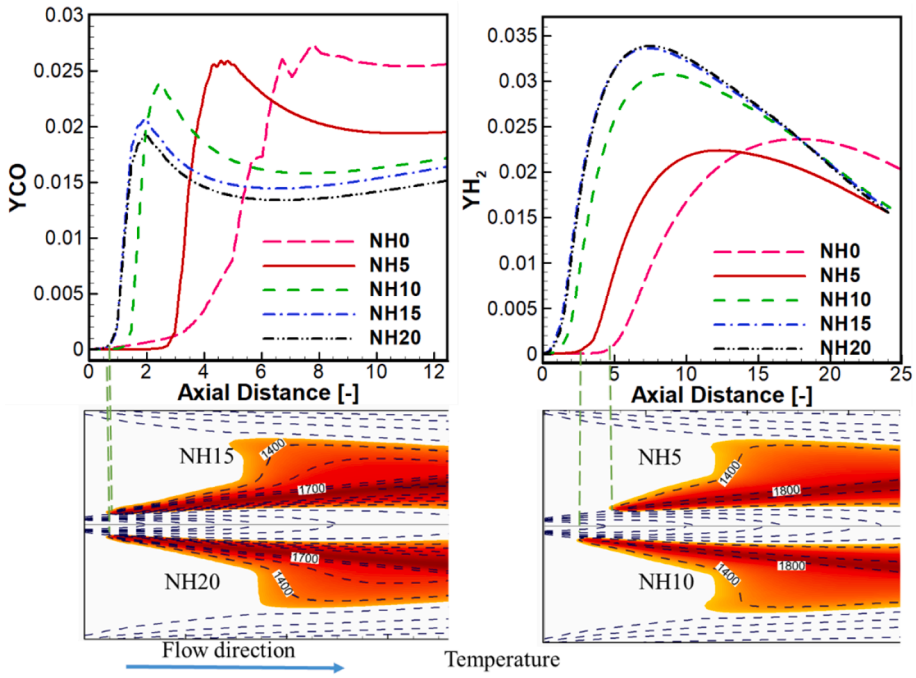

Fig. 5. Preheating zone length as a function of the NH_3 mass fraction (x-axis is normalized with the diameter of the inlet fuel nozzle).

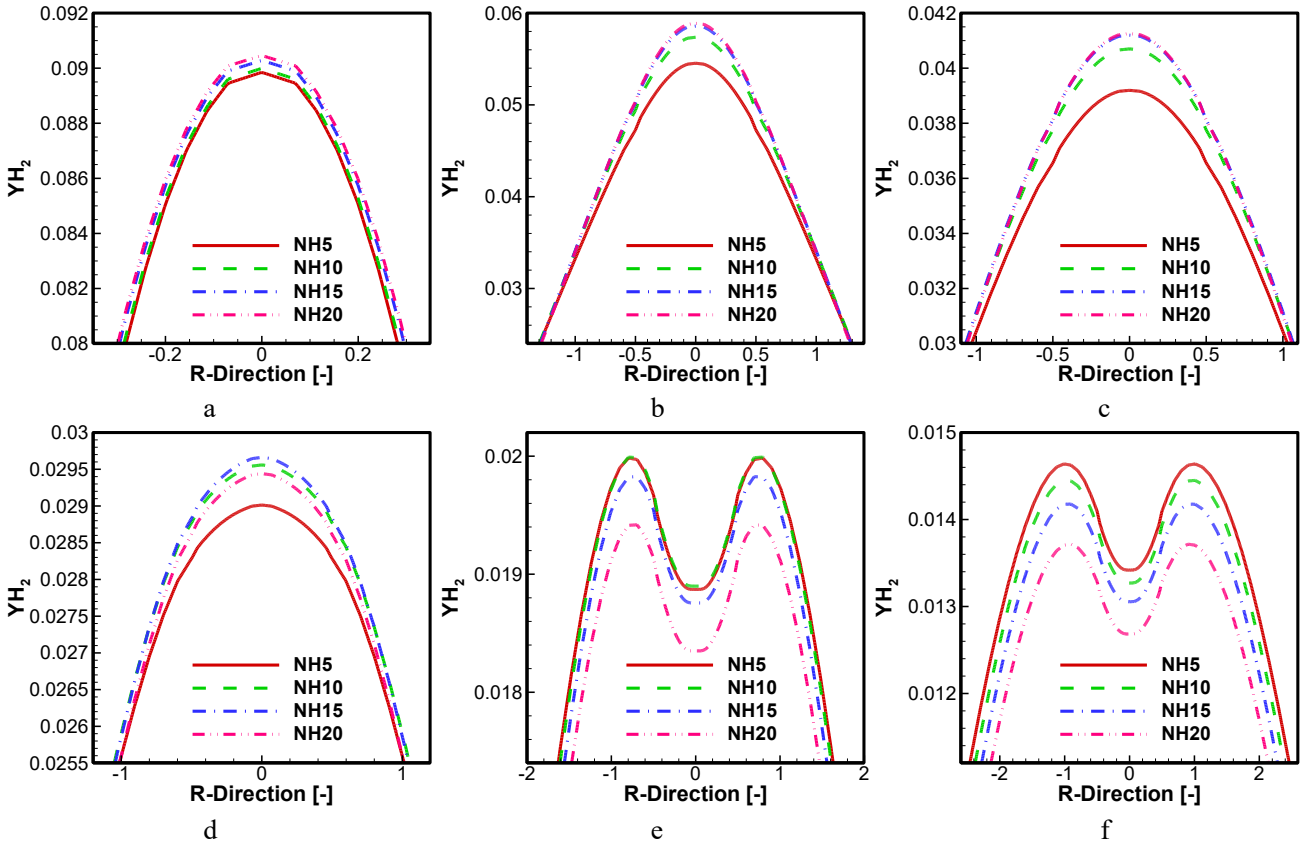

Fig. 6. Radial distribution of H_2 mass fraction in the axial distances of a- 0.01, b- 0.03, c-0.05, d = 0.07, e = 0.09, and f = 0.11 m (x-axis is normalized with the diameter of the inlet fuel nozzle).

acts as a flame marker, the weakened reaction area increases as the mass fraction of NH_3 increases in the zones far from the inlet.

In addition, changes in the fuel components affect the flow properties at the downstream of the reacting flow. One of these effects is related to changes in flow temperature, which lead to variation in the local density and viscosity of the reacting flow. These two properties change the kinematic viscosity of reacting flow. Local variations in flow density also change the local velocity through the mass conservation law, resulting in

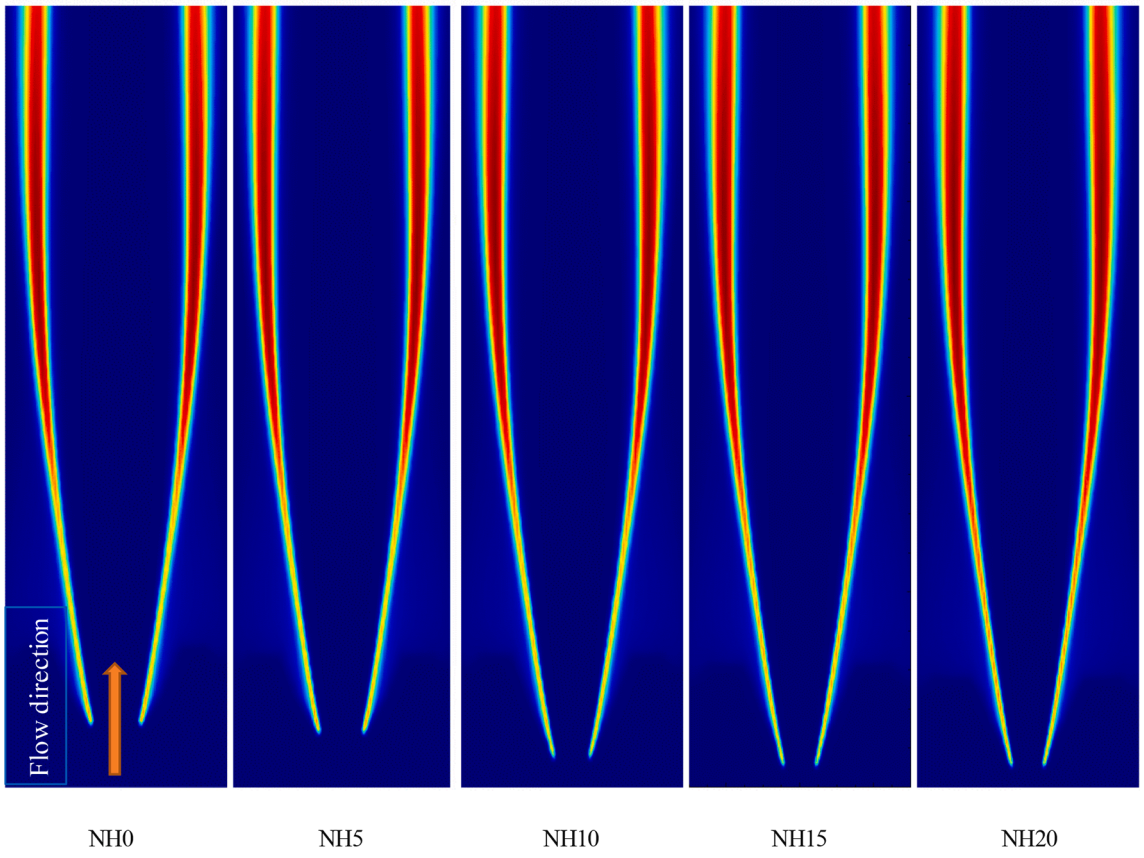

Fig. 7. Distribution of OH radical (starting point of OH production) for the cases shown in Table 4.

changes in the local flow dissipation rate. Followed by changes in local dissipation rate and kinematic viscosity, the local residence time of reacting flow is changed. Fig. 10 shows variations in the local ratio of kinematic viscosity and local turbulent dissipation rate as an index of the local flow residence time. It is evident that an increase in the mass fraction of NH_3 followed by a reduction of CH_4 in the fuel component leads to an enhancement of local residence time. It should be noted that combustion temperature depends on heat release, which has nonlinear behavior. Therefore, the changes in the local residence time should be nonlinear.

Fig. 11 represents the radial temperature and CO_2 mole fraction distribution for different mass fractions of NH_3. As shown in this figure, increasing the mass fraction of NH_3 along with decreasing the volume fraction of CH_4 decreases the process temperature. The maximum temperature of CH_4/H_2 combustion is about 60–80 K greater than that of $NH_3/CH_4/H_2$ (NH20) combustions under the same inlet condition (inlet velocity and temperature). This is due to enthalpy for the combustion of NH_3 being significantly less than that of CH_4, which results in less heat release per unit mass of the fuel burned. An important reason for the drop in the process temperature is the increase in nitrogen mass fraction due to addion of NH_3. Furthermore, changes in fuel components leads to changes in the heat capacity of the mixture as an important factor to change in process temperature. In addition, the drop in CO_2 mass fraction by reducing the methane content of the inlet fuel mixture decreases the overall emissivity of the reacting flow in the combustion process leading to a reduction of the radiation heat transfer. These explain the differences in the maximum process temperature at various axial distances. Nonetheless, the differences among the maximum temperatures at all axial distances of the computational domain were relatively small in MILD condition.

So far, it has been demonstrated that $NH_3/H_2/CH_4$ mixtures have lower flame temperatures (Fig. 11) and heat release rates than H_2/CH_4 mixtures (Fig. 8), and that the disparities increase as the NH_3 mass fraction increases. Due to the reduction of CH_4 mass fraction in the mixture brought about by an increase in NH_3 mass fraction, the carbon concentration falls, resulting in more available oxygen per carbon and a reduction of CO emissions by up to 15.3%. (see Fig. 12). In addition, the addition of NH_3 increases the mixture's residence time, allowing for more time for the mixture to react. Increasing the residence time by increasing the NH_3 mass fraction boosts the H_2O mass fraction production as a measure of combustion efficiency at a given axial location (Fig. 11) while adding NH_3 followed by reduction of CH_4 reduces H atoms, H_2O increases, meaning that the process is more completed. Therefore, adding NH_3 improves combustion efficiency and completeness.

In NH_3 flames, NO is produced mainly through the fuel NO pathway, and a higher NO concentration is anticipated in the reaction zone [71]. Fig. 13 depicts the radial distribution of NO and NO_2 mass fractions. According to Fig. 13, increasing the NH_3 mass fraction reduces the amount of NO_2 at the downstream at the axial distance of 0.2 m. This figure shows that by addition of NH_3, the amount of NO rapidly increases near the inlet nozzles. For instance, by adding only 5% of NH_3 mass fraction to the CH_4/H_2 blend, NO emission raised by several orders of magnitude reaching the unacceptable levels of 1000 ppm in the region near to the inlet nozzles. In general, the HNO intermediate channel is the major NO generation pathway in combustion of NH_3 [72]. Fig. 14 shows the dependency of HNO mass fraction to enhancement of NH_3 in the fuel blend. Addition of NH_3 enhances the HNO mass fraction sharply at the zone near the inlet nozzles with a trend similar to NO changes. However, in the upstream and after the axial distance of 0.3 m, both NO and HNO emissions become the same for all investigated cases. The process temperature could be reason for the existence of same trend in NO and HNO production for various cases downstream. According to Fig. 11, the downstream temperature is nearly equal for all cases,

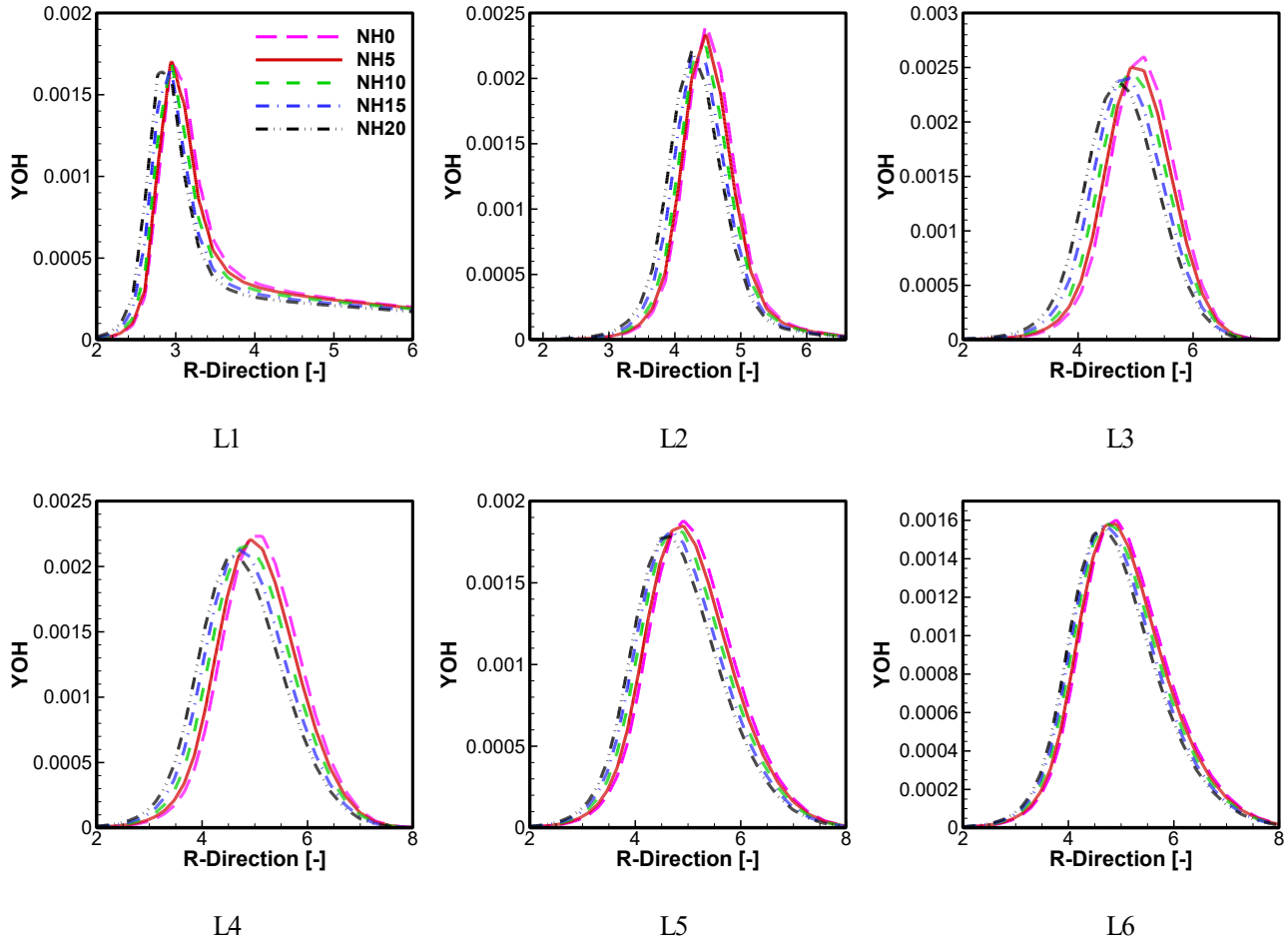

Fig. 8. Radial distribution of OH mass fraction in axial locations of L1 to L6 (x- axis is normalized with inlet fuel nozzle diameter).

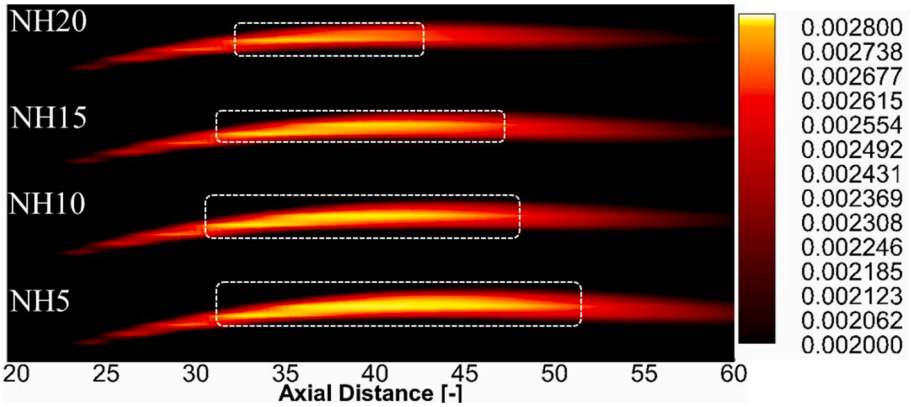

Fig. 9. The zone of maximum OH mass fraction in various cases showing the weakened reaction area (yellow color in cadre shows the OH maximum zone). (For interpretation of the references to color in this figure legend, the reader is referred to the web version of this article.)

resulting in similar NO production in all cases. In addition, the analyses show that because of dilution, the smaller O_2 mass fraction in the NH_3-MILD combustion leads to lower radical pool concentrations. Fig. 15 illustrates the radial distributions of the H/O mass fraction at different axial distances. Addition of NH_3 to the fuel blend reduces the concentration of both radicals slightly. It is known that H abstraction consumes NH_3 primary through the reaction with OH [1]. Other secondary consumption processes involve reactions with H and O, the most typical result of which is NH_2. Dependent mostly on concentration of the O/H radicals, NH_i (i = 0–2) oxidation can produce NO (through an HNO intermediate) or reduce NO (by NH_i + NO reactions) [73]. Therefore, the slight reduction of O/H radicals prevents NH_i radicals from increasing NO levels at the downstream. Since O/H radicals are reduced in the $NH_3/CH_4/H_2$ blends, and an increase in NH_3 further decreases these radicals in MILD regime, mixing of NH_3 with CH_4 and H_2 has no significant effect on NO concentration. In addition, the reduction of poor radicals inhibit the path $NH_2 \rightarrow HNO \rightarrow NO$ through $NH_2 + O <=> HNO + H$ which is the primary source of HNO [1]. Simultaneously, the reaction of $NH_2 + NO <=> N_2 + H_2O$ and the path of $NH_2 \rightarrow NNH \rightarrow N_2$ are intensified because the small O_2 mass fraction prevents the increase of

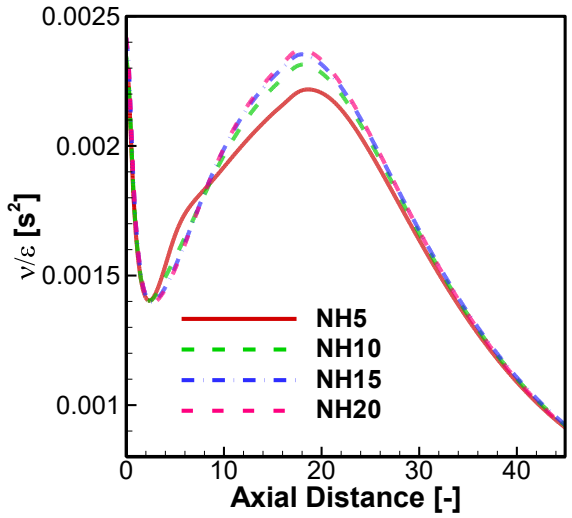

Fig. 10. Distribution of the ratio of local kinematic viscosity to local turbulent dissipation rate (x-axis is normalized with the diameter of the inlet fuel nozzle).

NO [26]. Furthermore, the analysis illustrates that the most important reaction for NO_2 generation is $NO + HO_2 = NO_2 + OH$. Since HO_2 is a common pre-ignition species that normally emerges in the low temperature region, this could explain the reduced NO_2 emission in high-temperature zones (see Fig. 13). It follows that MILD combustion technology could be a promising way of utilizing NH_3 as a carbon free fuel.

3. Conclusions

Numerical simulation of MILD combustion of $NH_3/H_2/CH_4$ blends, with relatively low concentration of ammonia, was carried out using k-ε turbulence model and modified EDC. Adequacy of the employed chemical mechanism and validity of the simulations were demonstrated. The effects of adding varying amounts of NH_3 to MILD combustion were then explored. The key findings of this study can be summarized as follows:

- When NH_3 is added to the MILD combustion regime, it significantly shortens the preheating zone and increases the reacting flow residence time, resulting in more complete combustion.
- The maximum temperature of CH_4/H_2 (NH0) combustion is approximately 60–80 K higher than that of $NH_3/CH_4/H_2$ (NH20).
- The addition of NH_3 decreases the CO emissions considerably and increases the NO at the inlet area. However, in the downstream, these emissions are roughly similar to those of H_2-CH_4 MILD combustion.
- Increasing the NH_3 mass fraction in the blended fuels decreases the flame lift-off and, unlike in conventional combustion, the addition of NH_3 to MILD combustion enhances the reactivity.
- Addition of NH_3 results in shrinkage of the zone of maximum mass fraction of OH, so the reaction zone is weaker.
- Adding NH_3 to CH_4/H_2 blend reduces the thickness of the reaction zone.

Finally, this work showed that MILD combustion could offer a promising route towards achieving clean combustion of ammonia. Further studies, particularly experimental investigations, are necessary to fully clarify this point.

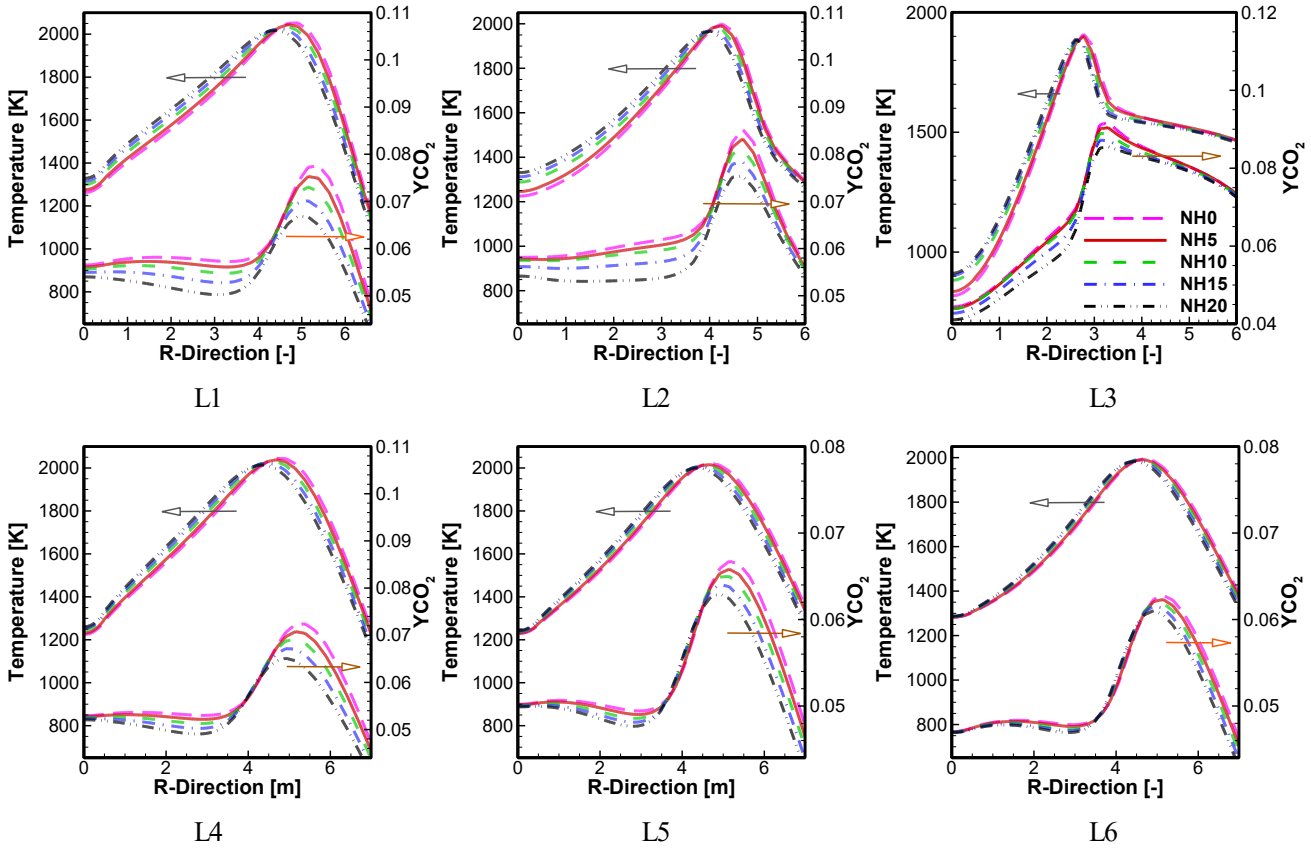

Fig. 11. Radial temperature and CO_2 mole fraction distributions for different cases in axial locations of L1 to L6 (x- axis is normalized with inlet fuel nozzle diameter).

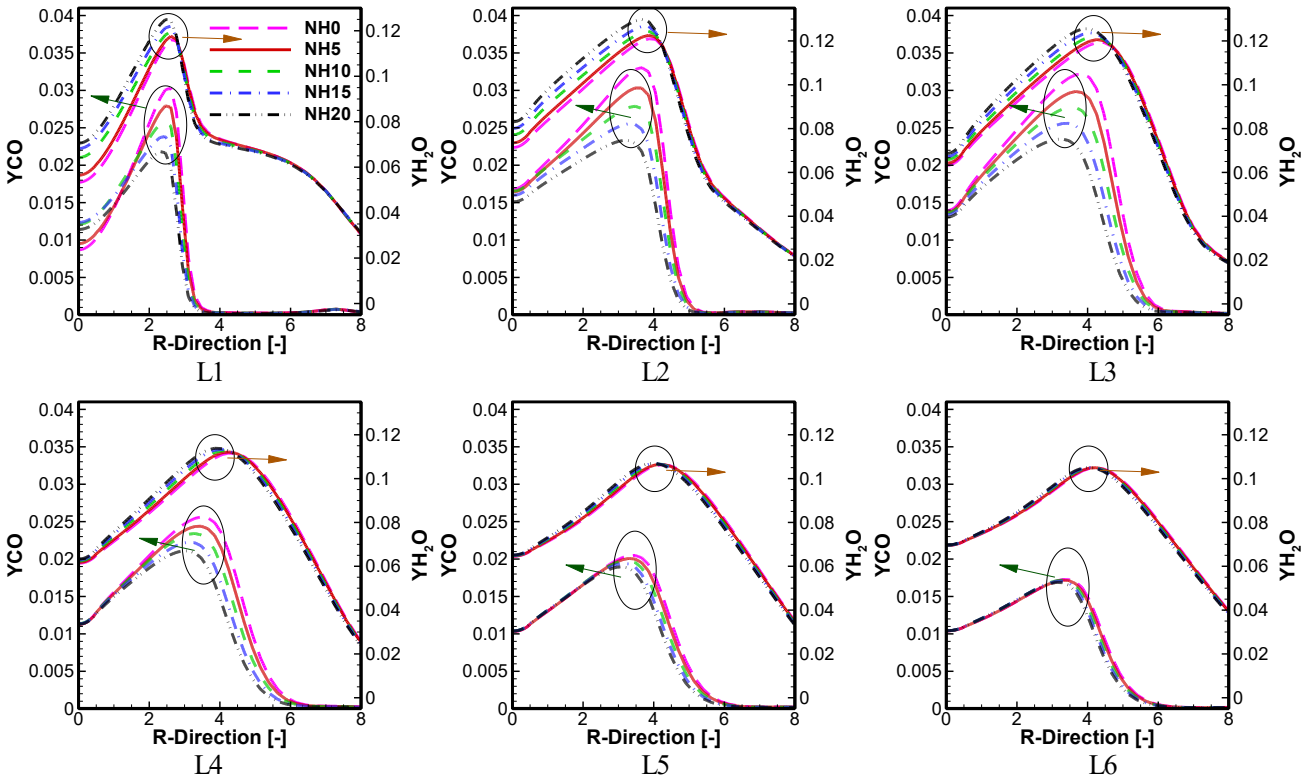

Fig. 12. Radial distributions of CO and H_2O mass fraction in axial locations of L1 to L6 (x- axis is normalized with inlet fuel nozzle diameter).

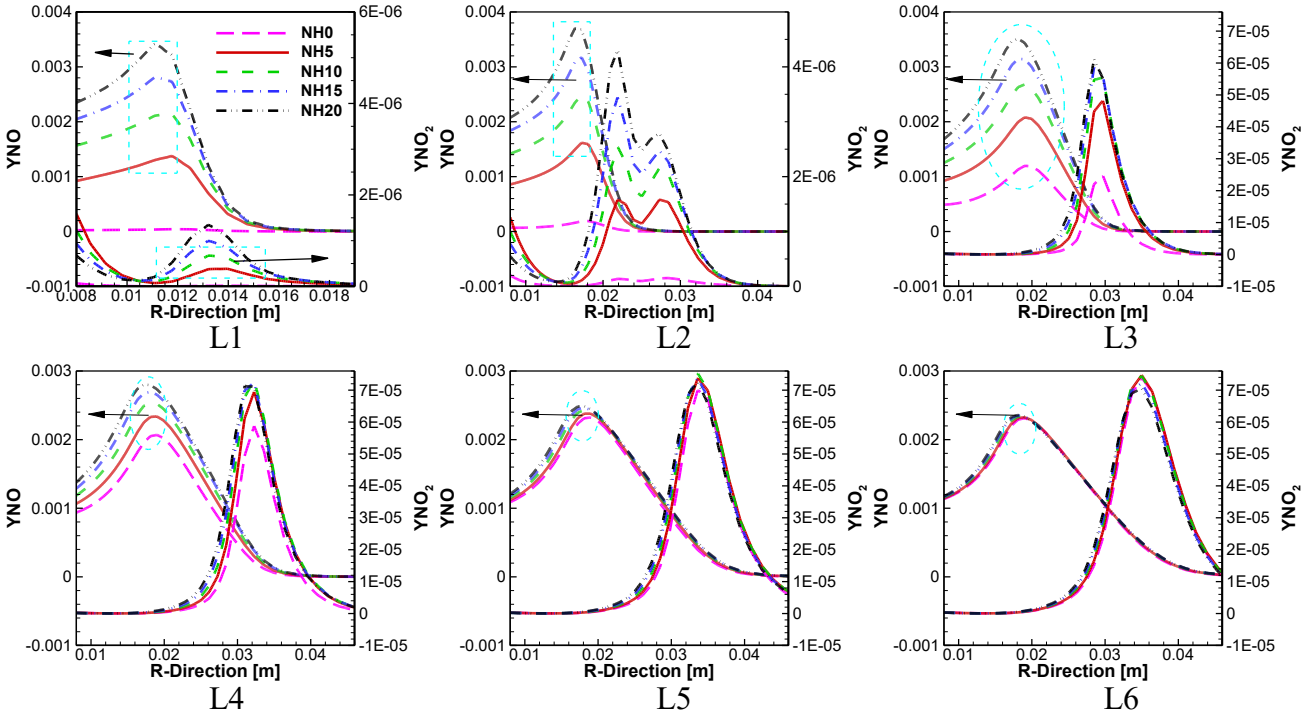

Fig. 13. The radial distribution of NO and NO_2 mass fractions in axial locations of L1 to L6 (x- axis is normalized with inlet fuel nozzle diameter).

CRediT authorship contribution statement

Seyed Mahmood Mousavi: Conceptualization, Methodology, Validation, Formal analysis, Investigation, Writing – original draft. **Freshteh Sotoudeh:** Conceptualization, Methodology, Validation, Formal analysis, Investigation, Writing – original draft. **Daeyoung Jun:** Software, Validation. **Bok Jik Lee:** Conceptualization, Methodology, Resources, Writing – review & editing. **Javad Abolfazli Esfahani:** Conceptualization, Writing – review & editing. **Nader Karimi:** Conceptualization, Writing – review & editing.

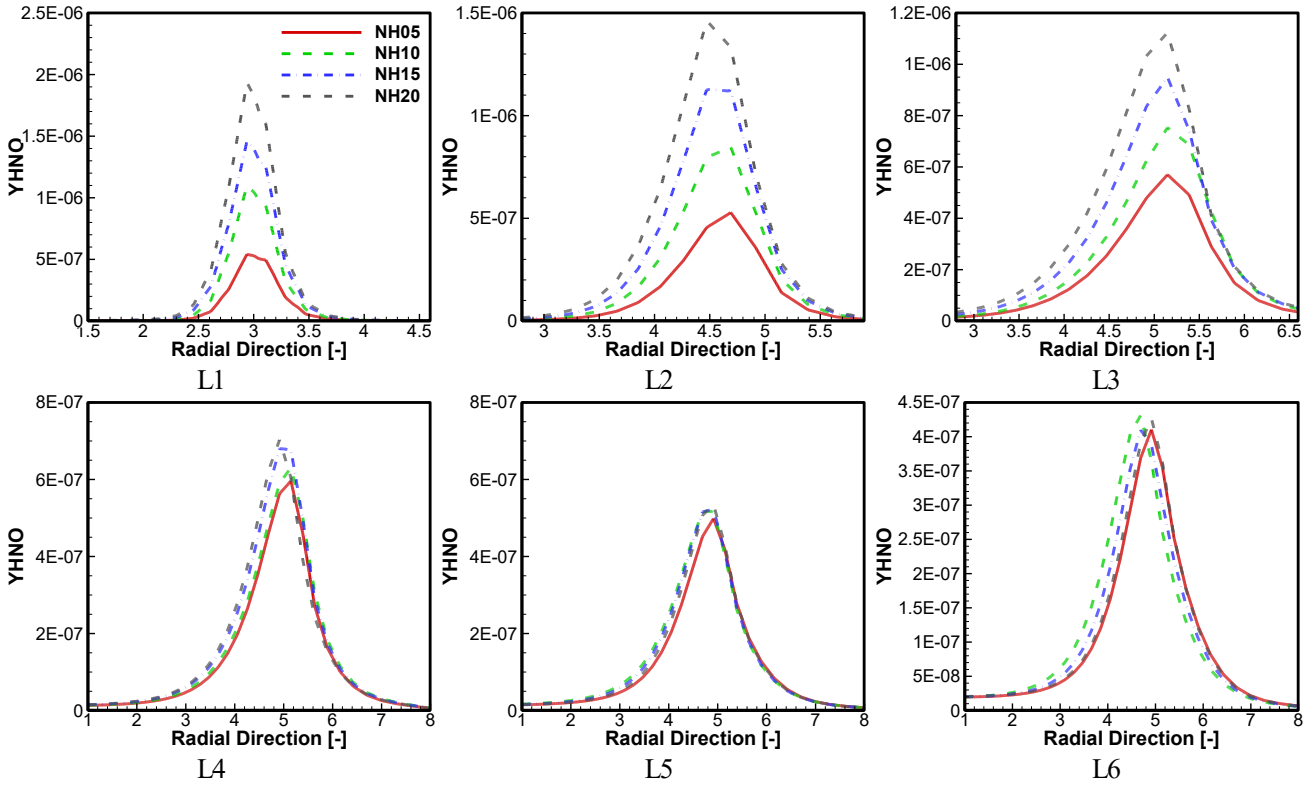

Fig. 14. Dependency of HNO mass fraction to enhancement of NH_3 in fuel blend in axial locations of L1 to L6 (x- axis is normalized with inlet fuel nozzle diameter).

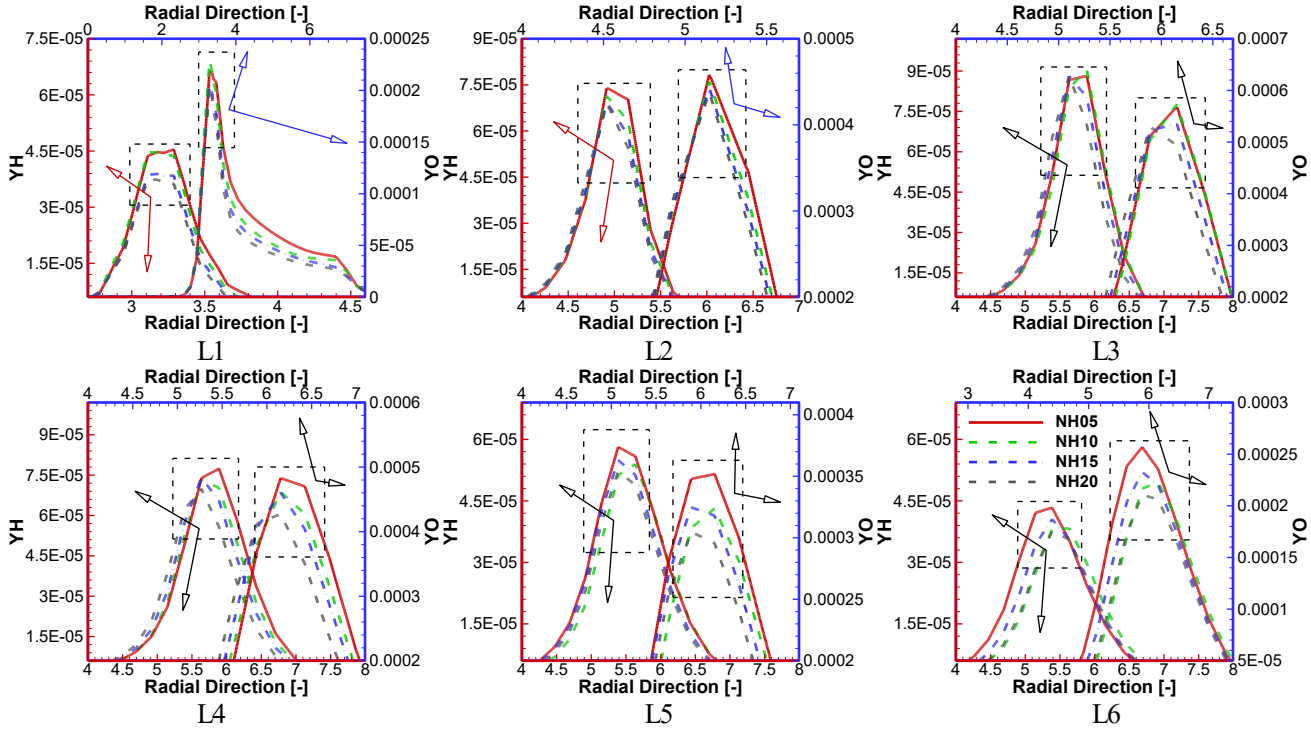

Fig. 15. Radial distribution of H and O mass fractions in axial locations of L1 to L6 (x- axis is normalized with inlet fuel nozzle diameter).

Declaration of Competing Interest

The authors declare that they have no known competing financial interests or personal relationships that could have appeared to influence the work reported in this paper.

Data availability

No data was used for the research described in the article.

Acknowledgements

This work was supported by the Korea Institute of Energy Technology Evaluation and Planning (KETEP) and the Ministry of Trade, Industry and Energy (MOTIE) of the Republic of Korea (No. 20181110100290). N. Karimi acknowledges the financial support provided by EPSRC (UK) through grant no. EP/V036777/1.

References

[1] Kobayashi H, Hayakawa A, Somarathne KDK, Okafor E. Science and technology of ammonia combustion. Proc Combust Inst 2019;37(1):109–33.
[2] Verkamp FJ, Hardin MC, Williams JR. Ammonia combustion properties and performance in gas-turbine burners. Symposium (Int) Combust 1967;11(1):985–92.
[3] Pratt D. Performance of ammonia-fired gas-turbine combustors. California Univ Berkeley Thermal Systems Div 1967.
[4] Valera-Medina A, Xiao H, Owen-Jones M, David WIF, Bowen PJ. Ammonia for power. Prog Energy Combust Sci 2018;69:63–102.
[5] Dimitriou P, Javaid R. A review of ammonia as a compression ignition engine fuel. Int J Hydrogen Energy 2020;45(11):7098–118.
[6] An Z, Zhang M, Zhang W, Mao R, Wei X, Wang J, et al. Emission prediction and analysis on CH4/NH3/air swirl flames with LES-FGM method. Fuel 2021;304:121370.
[7] Yin G, Wang C, Zhou M, Zhou Y, Hu E, Huang Z. Experimental and kinetic study on laminar flame speeds of ammonia/syngas/air at a high temperature and elevated pressure. Frontiers Energy 2021.
[8] Yin G, Li J, Zhou M, Li J, Wang C, Hu E, et al. Experimental and kinetic study on laminar flame speeds of ammonia/dimethyl ether/air under high temperature and elevated pressure. Combust Flame 2022;238:111915.
[9] Li J, Lai S, Chen D, Wu R, Kobayashi N, Deng L, et al. A review on combustion characteristics of ammonia as a carbon-free fuel. Front Energy Res 2021;9(602).
[10] Hayakawa A, Arakawa Y, Mimoto R, Somarathne KDKA, Kudo T, Kobayashi H. Experimental investigation of stabilization and emission characteristics of ammonia/air premixed flames in a swirl combustor. Int J Hydrogen Energy 2017;42(19):14010–8.
[11] Kurata O, Iki N, Matsunuma T, Inoue T, Tsujimura T, Furutani H, et al. Performances and emission characteristics of NH3–air and NH3CH4–air combustion gas-turbine power generations. Proc Combust Inst 2017;36(3):3351–9.
[12] Hayakawa A, Goto T, Mimoto R, Arakawa Y, Kudo T, Kobayashi H. Laminar burning velocity and Markstein length of ammonia/air premixed flames at various pressures. Fuel 2015;159:98–106.
[13] Ji L, Wang J, Hu G, Mao R, Zhang W, Huang Z. Experimental study on structure and blow-off characteristics of NH3/CH4 co-firing flames in a swirl combustor. Fuel 2022;314:123027.
[14] Mørch CS, Bjerre A, Gøttrup MP, Sorenson SC, Schramm J. Ammonia/hydrogen mixtures in an SI-engine: Engine performance and analysis of a proposed fuel system. Fuel 2011;90(2):854–64.
[15] Nozari H, Tuncer O, Karabeyoglu A. Evaluation of ammonia-hydrogen-air combustion in SiC porous medium based burner. Energy Procedia 2017;142:674–9.
[16] Valera-Medina A, Morris S, Runyon J, Pugh DG, Marsh R, Beasley P, et al. Ammonia, Methane and Hydrogen for Gas Turbines. Energy Procedia 2015;75:118–23.
[17] da Rocha RC, Costa M, Bai X-S. Chemical kinetic modelling of ammonia/hydrogen/air ignition, premixed flame propagation and NO emission. Fuel 2019;246:24–33.
[18] Han X, Wang Z, Costa M, Sun Z, He Y, Cen K. Experimental and kinetic modeling study of laminar burning velocities of NH3/air, NH3/H2/air, NH3/CO/air and NH3/CH4/air premixed flames. Combust Flame 2019;206:214–26.
[19] Filipe Ramos C, Rocha RC, Oliveira PMR, Costa M, Bai X-S. Experimental and kinetic modelling investigation on NO, CO and NH3 emissions from NH3/CH4/air premixed flames. Fuel 2019;254:115693.
[20] Zhu X, Khateeb AA, Guiberti TF, Roberts WL. NO and OH* emission characteristics of very-lean to stoichiometric ammonia–hydrogen–air swirl flames. Proc Combust Inst 2021;38(4):5155–62.
[21] Murakami Y, Nakamura H, Tezuka T, Hiraoka K, Maruta K. Effects of mixture composition on oxidation and reactivity of DME/NH3/air mixtures examined by a micro flow reactor with a controlled temperature profile. Combust Flame 2022;238:111911.
[22] Wünning JA, Wünning JG. Flameless oxidation to reduce thermal no-formation. Prog Energy Combust Sci 1997;23(1):81–94.
[23] Cavaliere A, de Joannon M. Mild combustion. Prog Energy Combust Sci 2004;30(4):329–66.
[24] Cavaliere A, de Joannon M, Sabia P, Sorrentino G, Ragucci R. 3 - Highly preheated lean combustion. In: Dunn-Rankin D, Therkelsen P, editors. Lean combustion. Second Edition. Boston: Academic Press; 2016. p. 63–109.
[25] Manna MV, Sabia P, Ragucci R, de Joannon M. Oxidation and pyrolysis of ammonia mixtures in model reactors. Fuel 2020;264:116768.
[26] Shi H, Liu S, Zou C, Dai L, Li J, Xia W, et al. Experimental study and mechanism analysis of the NOx emissions in the NH3 MILD combustion by a novel burner. Fuel 2022;310:122417.
[27] Sabia P, Sorrentino G, Ariemma GB, Manna MV, Ragucci R, de Joannon M. MILD Combustion and Biofuels: A Minireview. Energy Fuels 2021;35(24):19901–19.
[28] Ferrarotti M, Bertolino A, Amaduzzi R, Parente A. On the influence of kinetic uncertainties on the accuracy of numerical modeling of an industrial flameless furnace fired with NH3/H2 blends: A numerical and experimental study. Front Energy Res 2020;8.
[29] Sorrentino G, Sabia P, Bozza P, Ragucci R, de Joannon M. Low-NOx conversion of pure ammonia in a cyclonic burner under locally diluted and preheated conditions. Appl Energy 2019;254:113676.
[30] Ariemma GB, Sabia P, Sorrentino G, Bozza P, de Joannon M, Ragucci R. Influence of water addition on MILD ammonia combustion performances and emissions. Proc Combust Inst 2021;38(4):5147–54.
[31] Rocha RC, Costa M, Bai X-S. Combustion and emission characteristics of ammonia under conditions relevant to modern gas turbines. Combust Sci Technol 2021;193(14):2514–33.
[32] Sorrentino G, Sabia P, Ariemma GB, Ragucci R, de Joannon M. Reactive structures of ammonia MILD combustion in diffusion ignition processes. Front Energy Res 2021;9(659).
[33] Ariemma GB, Sorrentino G, Ragucci R, de Joannon M, Sabia P. Ammonia/methane combustion: stability and NOx emissions. Combust Flame 2022;241:112071.
[34] Zhao Z, Li X, Zhang Z, Zha X, Chen Y, Gao Ge, et al. Combustion regimes and fuel-NO mechanism of CH4/NH3 jet diffusion flames in hot O2/CO2 co-flow. Fuel Process Technol 2022;229:107173.
[35] Sun Z, Deng Y, Song S, Yang J, Yuan W, Qi F. Experimental and kinetic modeling study of the homogeneous chemistry of NH3 and NOx with CH4 at the diluted conditions. Combust Flame 2022:112015.
[36] Manna MV, Sabia P, Sorrentino G, Viola T, Ragucci R, de Joannon M. New insight into NH3-H2 mutual inhibiting effects and dynamic regimes at low-intermediate temperatures. Combust Flame 2022:111957.
[37] Mousavi SM, Kamali R, Sotoudeh F, Karimi N, Lee BJ. Numerical investigation of the plasma-assisted MILD combustion of a CH4/H2 fuel blend under various working conditions. J Energy Res Technol 2021;143(6):062302.
[38] Mousavi SM, Kamali R, Sotoudeh F, Karimi N, Jeung I-S. Numerical investigation of the effects of swirling hot co-flow on MILD combustion of a hydrogen-methane blend. J Energy Res Technol 2020;142(11).
[39] Swaminathan N. Physical insights on MILD combustion from DNS. Front Mech Eng 2019;5(59).
[40] Doan NAK, Swaminathan N. Role of radicals on MILD combustion inception. Proc Combust Inst 2019;37(4):4539–46.
[41] Lewandowski MT, Ertesvåg IS. Analysis of the Eddy Dissipation Concept formulation for MILD combustion modelling. Fuel 2018;224:687–700.
[42] Ferrarotti M, Li Z, Parente A. On the role of mixing models in the simulation of MILD combustion using finite-rate chemistry combustion models. Proc Combust Inst 2019;37(4):4531–8.
[43] Ertesvåg IS. Analysis of Some Recently Proposed Modifications to the Eddy Dissipation Concept (EDC). Combust Sci Technol 2020;192(6):1108–36.
[44] Lewandowski MT, Li Z, Parente A, Pozorski J. Generalised Eddy Dissipation Concept for MILD combustion regime at low local Reynolds and Damköhler numbers. Part 2: Validation of the model. Fuel 2020;278:117773.
[45] Ertesvåg IS. Scrutinizing proposed extensions to the Eddy Dissipation Concept (EDC) at low turbulence Reynolds numbers and low Damköhler numbers. Fuel 2022;309:122032.
[46] Cuoci A, Frassoldati A, Faravelli T, Ranzi E. OpenSMOKE++: An object-oriented framework for the numerical modeling of reactive systems with detailed kinetic mechanisms. Comput Phys Commun 2015;192:237–64.
[47] Parente A, Malik MR, Contino F, Cuoci A, Dally BB. Extension of the Eddy Dissipation Concept for turbulence/chemistry interactions to MILD combustion. Fuel 2016;163:98–111.
[48] Lewandowski MT, Pozorski J. Assessment of turbulence-chemistry interaction models in the computation of turbulent non-premixed flames. J Phys: Conf Ser 2016;760:012015.
[49] De A, Dongre A. Assessment of turbulence-chemistry interaction models in MILD combustion regime. Flow Turbul Combust 2015;94(2):439–78.
[50] ErtesvÅG IS, Magnussen BF. The Eddy Dissipation turbulence energy cascade model. Combust Sci Technol 2000;159(1):213–35.
[51] De A, Oldenhof E, Sathiah P, Roekaerts D. Numerical simulation of delft-jet-in-hot-coflow (DJHC) flames using the Eddy dissipation concept model for turbulence-chemistry interaction. Flow Turbul Combust 2011;87(4):537–67.
[52] Li Z, Cuoci A, Sadiki A, Parente A. Comprehensive numerical study of the Adelaide Jet in Hot-Coflow burner by means of RANS and detailed chemistry. Energy 2017;139:555–70.
[53] Li Z, Malik MR, Cuoci A, Edcsmoke PA. A new combustion solver for stiff chemistry based on OpenFOAM®. AIP Conf Proc 2017;1863.
[54] Dally BB, Karpetis AN, Barlow RS. Structure of turbulent non-premixed jet flames in a diluted hot coflow. Proc Combust Inst 2002;29(1):1147–54.
[55] Christo FC, Dally BB. Modeling turbulent reacting jets issuing into a hot and diluted coflow. Combust Flame 2005;142(1):117–29.
[56] Mardani A, Tabejamaat S, Ghamari M. Numerical study of influence of molecular diffusion in the Mild combustion regime. Combust Theor Model 2010;14(5):747–74.
[57] Frassoldati A, Sharma P, Cuoci A, Faravelli T, Ranzi E. Kinetic and fluid dynamics modeling of methane/hydrogen jet flames in diluted coflow. Appl Therm Eng 2010;30(4):376–83.
[58] Mousavi SM, Kamali R, Sotoudeh F, Pourabidi R, Karimi N, Jeung I-S. A comprehensive investigation of acoustic power level in a moderate or intense low oxygen dilution in a jet-in-hot-coflow under various working conditions. Aerosp Sci Technol 2019;93:105339.

[59] Tu Y, Liu H, Yang W. Flame characteristics of CH4/H2 on a jet-in-hot-coflow burner diluted by N2, CO2, and H2O. Energy Fuels 2017;31(3):3270–80.
[60] Li R, Konnov AA, He G, Qin F, Zhang D. Chemical mechanism development and reduction for combustion of NH3/H2/CH4 mixtures. Fuel 2019;257:116059.
[61] Poinsot T, Veynante D. Theoretical and numerical combustion. RT Edwards, Inc; 2005.
[62] Mousavi SM, Roohi E. Large eddy simulation of shock train in a convergent–divergent nozzle. Int J Mod Phys C 2013;25(04):1450003.
[63] Song Y, Marrodán L, Vin N, Herbinet O, Assaf E, Fittschen C, et al. The sensitizing effects of NO2 and NO on methane low temperature oxidation in a jet stirred reactor. Proc Combust Inst 2019;37(1):667–75.
[64] Stagni A, Cavallotti C, Arunthanayothin S, Song Yu, Herbinet O, Battin-Leclerc F, et al. An experimental, theoretical and kinetic-modeling study of the gas-phase oxidation of ammonia. React Chem Eng 2020;5(4):696–711.
[65] Okafor EC, Naito Y, Colson S, Ichikawa A, Kudo T, Hayakawa A, et al. Measurement and modelling of the laminar burning velocity of methane-ammonia-air flames at high pressures using a reduced reaction mechanism. Combust Flame 2019;204:162–75.
[66] Gregory PSDMG, Michael F, Nigel WM, Boris E, Mikhail G, Thomas Bowman C, Ronald KH, Soonho S, William CG, Jr., Vitali VL, Zhiwei Q. http://www.me.berkeley.edu/gri_mech/.
[67] Mazzone S, Campbell A, Zhang G, García-García FR. Ammonia cracking hollow fibre converter for on-board hydrogen production. Int J Hydrogen Energy 2021;46(76):37697–704.
[68] Alboshmina N. Ammonia cracking with heat transfer improvement technology. Cardiiff University; 2019.
[69] Zharfa M, Karimi N. Intensification of MILD combustion of methane and hydrogen blend by the application of a magnetic field- a numerical study. Acta Astronaut 2021;184:259–68.
[70] Medwell PR, Kalt PAM, Dally BB. Reaction zone weakening effects under hot and diluted oxidant stream conditions. Combust Sci Technol 2009;181(7):937–53.
[71] Hayakawa A, Goto T, Mimoto R, Kudo T, Kobayashi H. NO formation/reduction mechanisms of ammonia/air premixed flames at various equivalence ratios and pressures. Mech Eng J 2015;2(1):14–00402.
[72] Shrestha KP, Seidel L, Zeuch T, Mauss F. Detailed kinetic mechanism for the oxidation of ammonia including the formation and reduction of nitrogen oxides. Energy Fuels 2018;32(10):10202–17.
[73] Glarborg P, Miller JA, Ruscic B, Klippenstein SJ. Modeling nitrogen chemistry in combustion. Prog Energy Combust Sci 2018;67:31–68.